Role of control constraints in quantum optimal control

Dmitry V. Zhdanov and Tamar Seideman

Phys. Rev. A **92**, 052109 — Published 13 November 2015

DOI: 10.1103/PhysRevA.92.052109

Role of control constraints in quantum optimal control

Dmitry V. Zhdanov* and Tamar Seideman†
Department of Chemistry, Northwestern University, Evanston, IL 60208 USA

The problems of optimizing the value of an arbitrary observable of the two-level system at both a fixed time and the shortest possible time is theoretically explored. Complete identification and classification along with comprehensive analysis of globally optimal control policies and traps (i.e. policies which are locally but not globally optimal) is presented. The central question addressed is whether the control landscape remains trap-free if control constraints of the inequality type are imposed. The answer is astonishingly controversial: Although the traps are proven to always exist in this case, in practice they become trivially escapable once the control time is fixed and chosen long enough.

PACS numbers: 03.65.-w, 02.30.Yy, 03.67.Ac, 37.10.Jk

I. INTRODUCTION

Within the optimal control paradigm, efficient control of quantum dynamics is based on determination of the global maximum of the multidimensional "control landscape" with respect to the shapes of driving laser pulses or external magnetic fields. In the laboratory, the search usually involves sophisticated genetic algorithms [1]. This is a time-consuming procedure but it guarantees that the optimization will neither get "trapped" in the landscape's sub-optimal local extrema nor faltered in the vicinity of a saddle point. The existence of "traps" is known both experimentally and theoretically [1–3]. At the same time, there are strong arguments that a large variety of control problems may be treated as trap-free from the practical perspective [4–9]. These arguments, however, assume the set of controls to be an open manifold. In practice, this is not the case: The magnitudes of applied fields are constrained by a number of competing strong-field processes (ionization, dissociation) and to a lesser extent by technical limitations. The overall effect of these constraints on the landscape topology is an open question. They are known, however, to dramatically influence the forms of the time-optimal controls (see e.g. [10–12]), which are highly relevant for quantum information applications.

In this paper we study in detail the constrained control landscape of the two-level Landau-Zener system representing the probably most fundamental model of a controlled qubit with a single control parameter, denoted below u. The corresponding master equation reads as

$$\rho(\tau)=U_{\tau,0}(u)\rho(0)U^{\dagger}_{\tau,0}(u), \tag{1}$$

with the unitary transformation $U_{\tau'',\tau'}(u)$ defined as $U_{\tau'',\tau'}(u)=\overrightarrow{\exp}(-i\int_{\tau=\tau'}^{\tau''}(\hat{\sigma}_x+u(\tau)\hat{\sigma}_z)d\tau)$. Here ρ is the system's density matrix, σ_x and σ_z are Pauli matrices, τ is a dimensionless time $\tau=\alpha t$, and the control parameter is usually proportional to the interaction strength with an external controlled electric or magnetic field ($u=\beta\mathcal{E}$ or $u=\beta\mathcal{B}$). Depending on the physical meaning of the scaling factors α and β, Eq. (1) can represent the wide variety of modern experiments, including magnetic and\or optical control of quantum dots [13], vacancy centers in crystals [14], spin states of atoms and molecules [12], Bose-Einstein condensates [15, 16] and superconducting circuits [17].

We consider the following optimal control problem:

$$J=\mathrm{Tr}[\rho(T)\hat{O}]\rightarrow \max; \tag{2}$$

$$-u_{\max}\leq u\leq u_{\max}; \tag{3}$$

$$T<T_{\max}, \tag{4}$$

where maximization is with respect to the program (or control policy) $\tilde{u}(\tau)$, and possibly also the final time T. In the context of qubit design, for instance, the performance index (2) with $\hat{O}=|1\rangle\langle 1|$ can represent the task of initial preparation of the qubit in a given initial pure state $|1\rangle$. Provided that the initial state of the system is $|0\rangle$ ($\langle 0|1\rangle=0$), the optimal policy will effectively represent the realization of the SWAP quantum gate (up to undefined diagonal phase shifts). In this case, the bound (4) is motivated by the unrecoverable losses of operation fidelity due to uncontrollable decoherence at long times.

The key question of our study is the extent to which the restrictions (3), (4) complicate finding the policy $\tilde{u}^{\rm opt}(\tau)$ that maximizes the functional $J[u(t)]$ (representing the system's control landscape) using local search methods. The Landau-Zener system is special from this perspective since it is the only system for which the absence of traps in the unconstrained case (i.e. when $u_{\max}=\infty$ in (3)) was formally proven [18–20]. Moreover, its complete controllability for any finite value of $u_{\max}$ (provided that $T_{\max}$ is chosen sufficiently long) was also justified [21–23]. Thus, this system provides opportunity to evaluate the effect of constraints (3) and (4) on the landscape complexity in the most pristine form. The existing data portend that this effect should be nontrivial. For example, the unconstrained time-optimal policies $\tilde{u}(\tau)$ are shown to be $\tilde{u}(\tau)=c'\delta(\tau)+c''\delta(\tau-T)$ where c' and c'' are constants and $\delta(\tau)$ is the Dirac delta function [25]. Such

* dm.zhdanov@gmail.com
† t-seideman@northwestern.edu

solutions are evidently inconsistent with any constraints of the form (3).

An additional feature of the Landau-Zener system is its simplicity, which allows us to analytically infer the topology of $J[u]$. At the same time, this system constitutes an elementary building block for describing the dynamics of a variety of important quantum systems, from NMR controlled spin chains to laser-driven excitations in atoms, molecules and quantum dots. These features make the Landau-Zener system a lovely model whose analytical beauty could help to understand the fundamental controllability and regularity properties of generic quantum control.

It is worth noting that the restrictions (3) are critical in the foundation of modern theory of optimal control since the corresponding problems can not be solved in the framework of classical calculus of variations and require special methods, such as the Pontryagin's maximum principle (PMP) [10, 11]. For completeness of the presentation, we provide in Sec. II and Appendix A a brief review of PMP and the known results of first-order analysis of the controlled Landau-Zener system in the PMP framework. In particular, we clarify why the unconstrained problem (2) is trap-free, and introduce the primary classification of the stationary points (i.e. the locally and globally optimal solutions, traps and saddle points) by showing that, in the case of time-optimal control, all of them, and likewise traps and saddle points in the case of fixed time control, are represented by piecewise-constant controls $\tilde{u}(\tau)$ that can take only 3 values: 0 and $\pm u_{\max}$.

The rest of the paper is organized as follows. In Sec. III we derive a comprehensive set of criteria that allow to outline the landscape profile and distinguish among its various types of stationary points. The obtained criteria substantially extend, generalize or specialize a number of known results [24–27] obtained for related problems using the index theory [28] or methods of optimal syntheses on 2-D manifolds [29]. In this work we propose the technique of "sliding" variations, which allows to reduce the high-order analysis to methodologically simple and intuitively appealing geometrical arguments.

In sections IV and V we apply these criteria to identify and classify the traps and saddle points for the cases of time-optimal and time-fixed control, respectively. A brief summary of the obtained results and the general conclusions that follow from this analysis are given in the final section VI.

We recommend readers who are interested primarily in physical rather than formal mathematical content of the paper to skip directly to concluding section VI after reviewing Section II and Appendix A, and then, if necessary, refer to sections III–V for details. For convenience, the key results of the these sections are compactly formulated in the form of 16 propositions whose proofs are deferred to Appendices B–J.

II. REGULAR AND SINGULAR OPTIMAL POLICIES

In this section, we review the first-order analysis of problem (1) with constraint (3) in the PMP framework. For completeness, we sketch in more detail the basics of the Pontryagin theory and outline the derivations of key statements and relations of this section in Appendix A. For further details, we refer interested readers to the extensive literature on this topic, e.g. [11], pp.280-286, [24]. PMP provides the necessary criterion of local optimality of control $u(\tau)$ in terms of the Hamilton-type Pontryagin function $K(\rho(\tau), \hat{O}(\tau), u(\tau))$,

$$\tilde{\mathbf{u}}(\tau) = \arg\max_{u(\tau)} K(\tilde{\rho}(\tau), \tilde{\hat{O}}(\tau), u(\tau)). \tag{5}$$

Here the matrix elements of the operator $\tilde{\hat{O}}$ represent the set of so-called costate (or adjoint) variables (see Appendix A). The processes satisfying the PMP are called stationary points, or extremals, and will be denoted by $\tilde{:}$ $\{\tilde{u}(\tau), \tilde{\rho}(\tau), \tilde{\hat{O}}(\tau)\}$.

The explicit form of the Pontryagin function of the control problem (1), (2) is

$$K(\rho(\tau), \hat{O}(\tau), u(\tau)) = -i \operatorname{Tr}\left\{[\rho(\tau), \hat{O}(\tau)](\hat{\sigma}_x + u(\tau)\hat{\sigma}_z)\right\}, \tag{6}$$

the evolution equation for $\hat{O}(\tau)$ coincides with (1),

$$\hat{O}(\tau'') = U_{\tau'',\tau'}(u)\hat{O}(\tau')U^{\dagger}_{\tau'',\tau'}(u), \tag{7}$$

and the boundary conditions read as

$$\hat{O}(T) = \hat{O}; \tag{8}$$

$$K(T)\begin{cases} =0 & \text{if } T \text{ is unconstrained;} \\ \geq 0 & \text{in the case (4).} \end{cases} \tag{9}$$

Since the Pontryagin function (6) depends linearly on $u(\tau)$, the PMP can be satisfied in two ways:

1) The switching function $\frac{\partial}{\partial u(\tau)} K = -i \operatorname{Tr}\left\{[\rho(\tau), \hat{O}(\tau)]\hat{\sigma}_z\right\} \neq 0$, and $\tilde{u}(\tau) = u_{\max}\operatorname{sign}(\frac{\partial}{\partial u(\tau)} K)$. The corresponding section of the trajectory is called regular. In this case the optimal policy $\tilde{u}(\tau)$ is actively constrained, so that relaxing the constraints (3) will improve the optimization result. For this reason, the optimal trajectory containing the regular sections can not be kinematically optimal. An optimal process $\{\tilde{\rho}(\tau), \tilde{\hat{O}}(\tau), \tilde{u}(\tau)\}$ for which $\tilde{u}(\tau) = \pm u_{\max}$ everywhere except for a finite number of time moments is often referred to as bang-bang control.

2) It may happen that the switching function remains equal to zero over a finite interval of time. The corresponding segment of the trajectory is called singular,

and the associated optimal control can be determined only from higher-order optimality criteria, such as the generalized Legendre-Clebsch conditions or Goh condition [11, 30, 31].

Substituting (1) and (7) into (6), one can directly check that the Pontryagin function for problem (1) is constant along any extremal,

$$\forall\tau : K(\tau){=}\tilde{K}{\geq}0 \text{ on each extremal,} \tag{10}$$

where the strict inequality holds only if the constraint (4) is active, and

$$\forall\tau : K(\tau){\equiv}0 \text{ for any kinematically optimal solution.} \tag{11}$$

A. Singular extremals of the problem (1)

Every kinematically optimal solution $\tilde{u}(\tau)$ consist of a single singular subarc. Here we show that in the case of the Landau-Zener system the converse is also true: every singular extremal $\tilde{u}(\tau)$ corresponding to an inactive constraint (4) delivers the global kinematic extremum (maximum or minimum) to the problem (2). Indeed, let τ_1 be an arbitrary internal point of the singular trajectory. The PMP states that

$$\frac{\partial}{\partial u(\tau)}\,K(\tau){=}{-}i\,\mathrm{Tr}\left\{[\rho(\tau_1),\hat{O}(\tau_1)]U^{\dagger}_{\tau,\tau_1}(\tilde{u})\hat{\sigma}_z U_{\tau,\tau_1}(\tilde{u})\right\}\equiv 0 \tag{12}$$

for any τ such that $|\tau-\tau_1|{<}\epsilon$ for a sufficiently small ϵ. In particular,

$$-i\,\mathrm{Tr}\left\{[\rho(\tau_1),\hat{O}(\tau_1)]\hat{\sigma}_z\right\}{=}0. \tag{13a}$$

The two subsequent time derivatives of the equality (12) at $\tau{=}\tau_1$ give

$$-i\,\mathrm{Tr}\left\{[\rho(\tau_1),\hat{O}(\tau_1)]\hat{\sigma}_y\right\}{=}0; \tag{13b}$$

$$-i\tilde{u}(\tau_1)\,\mathrm{Tr}\left\{[\rho(\tau_1),\hat{O}(\tau_1)]\hat{\sigma}_x\right\}{=}0. \tag{13c}$$

Equations (13) can be simultaneously satisfied only in two cases:

$$[\rho(\tau),\hat{O}(\tau)]{=}0; \tag{14a}$$

$$[\rho(\tau),\hat{O}(\tau)]{=}i\kappa\hat{\sigma}_x \quad\text{and}\quad u(\tau){=}0 \quad (\kappa{=}\mathrm{const}{\neq}0). \tag{14b}$$

The condition (14a) is nothing but the criterion of the global kinematic extremum (maximum or minimum) for our two-level system. In other words, we showed that all the extrema of the landscape $J(u)$ for the unconstrained Landau-Zener system except for the case of $u(t){\equiv}0$ are its global kinematic maxima and minima. This result was obtained in [18, 19].

The condition (14b) indicates that the only possible everywhere singular non-kinematic extremal of the problem (2) is $\tilde{u}(\tau){\equiv}0$ ($\tau{\in}[0,T]$). Eq. (6) implies that $K(\tau){=}\kappa$ in this case. Thus, in view of (9), this extremal can appear only when the constraint (4) is active.

B. Regular and mixed extremals of the problem (1)

According to the PMP and conditions (14), the generic non-singular extremal is the piecewise-constant function with n switchings of either bang ($u{=}{\pm}u_{\max}$) or bang-singular ($u{=}{\pm}u_{\max},0$) type, where the singular arcs match (14b). For brevity, we will refer to extremals with (without) singular arcs as of type II (type I). We will use the subscript i (i.e. $\tilde{\tau}_i$, $\tilde{\rho}_i$ etc., $0{<}i{<}n{+}1$) for the parameters related to the i-th control discontinuity (corner point). The durations of the right (left) adjacent arcs and the associated values of u will be labeled $\tilde{\Delta\tau}_i$ ($\tilde{\Delta\tau}_{i-1}$) and $\tilde{u}_i^+$ ($\tilde{u}_i^-$). The subscripts $i{=}0$ and $i{=}n{+}1$ will be reserved for the parameters of the trajectory endpoints. We will also sometimes use the notations ^{s}I and ^{s}II with index s denoting the number of times the control changes sign.

Let us first address the properties of type I extremals. The necessary condition of the i-th corner point is given by eq. (13a). Combining it with (10) we get

$$-i[\tilde{\rho}(\tilde{\tau}_i),\tilde{\hat{O}}(\tilde{\tau}_i)]{=}c_{i,1}\hat{\sigma}_x{+}c_{i,2}\hat{\sigma}_y, \quad c_{i,1},c_{i,2}\in\mathbb{R}, \tag{15}$$

where $c_{i,1}{=}0({>}0)$ when the constraint (4) is inactive(active) and the case $c_{i,1}{\leq}0$ can result from optimization with a fixed T. Consider the adjacent $(i{+}1)$-th bang arc. The PMP criterion (5) for its interior reads as

$$\tilde{u}(\tau)|_{\tau>\tilde{\tau}_i}{=}\arg\max_u \mathrm{Tr}[U_{\tau,\tilde{\tau}_i}(c_{i,1}\hat{\sigma}_x{+}c_{i,2}\hat{\sigma}_y)U^{-1}_{\tau,\tilde{\tau}_i}\hat{\sigma}_z]u, \tag{16}$$

which gives $\tilde{u}_i^+{=}\frac{c_{i,2}}{|c_{i,2}|}u_{\max}$. If the $(i{+}1)$-th arc ends with another corner point $\tilde{\tau}_{i+1}$, then it follows from (16) that

$$\mathrm{Tr}[U_{\tilde{\tau}_{i+1},\tilde{\tau}_i}(c_{i,1}\hat{\sigma}_x{+}c_{i,2}\hat{\sigma}_y)U^{-1}_{\tilde{\tau}_{i+1},\tilde{\tau}_i}\hat{\sigma}_z]{=}0. \tag{17}$$

Condition (17) can be reduced to

$$c_{i,2}\sqrt{u^2_{\max}{+}1}{=}{-}c_{i,1}\tilde{u}_i^+\tan(\tilde{\Delta\tau}_i\sqrt{u^2_{\max}{+}1}) \tag{18}$$

and resolved relative to $\Delta\tau_{i+1}$. Retaining the physically appropriate solutions consistent with eq. (16) we obtain:

$$\tilde{\Delta\tau}_{i+1}{=}\begin{cases}\tilde{\delta\tau}_i, & c_{i,1}{<}0;\\ \pi\cos(\alpha){-}\tilde{\delta\tau}_i, & c_{i,1}{>}0,\end{cases} \tag{19}$$

where $\alpha{=}\arctan(u_{\max})$ and

$$\tilde{\delta\tau}_i{=}\arctan\left(\left|\frac{c_{2,i}}{c_{1,i}u_{\max}}\right|\sec(\alpha)\right)\cos(\alpha). \tag{20}$$

Note that $-i[\tilde{\rho}(\tilde{\tau}_{i+1}),\tilde{\hat{O}}(\tilde{\tau}_{i+1})]{=}c_{1,i}\hat{\sigma}_x{-}c_{i,2}\hat{\sigma}_y$, i.e.

$$c_{1,i+1}{=}c_{1,i}, \quad c_{2,i+1}{=}{-}c_{2,i}. \tag{21}$$

Since eqs. (19) and (20) do not depend on the sign of $c_{i,2}$, one obtains that the durations of all interior bang segments are equal: $\forall i{\geq}1, i{<}n$: $\tilde{\Delta\tau}_i{=}\tilde{\Delta\tau}$ (see Fig. 1a). Moreover, eq. (19) admits the estimate

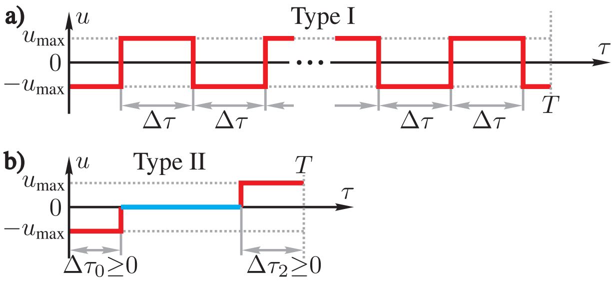

FIG. 1. Possible types of extremals $\tilde{u}(t)$ associated with non-kinematic optimal solutions and traps along with the locally time-optimal kinematic optimal solutions.

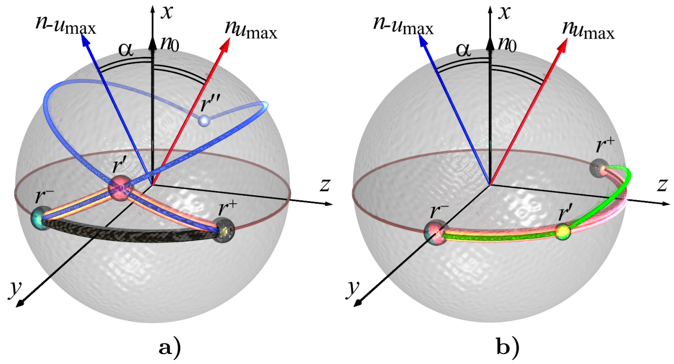

FIG. 2. (a) The case $r_y^- r_y^+ > 0$: The equatorial singular arc $r^- \to r^+$ (thick black line) is more time-effective than the bang-bang extremal $r^- \to r' \to r^+$ (thick orange line). The extremal $r^- \to r'' \to r^+$ (thin blue curve) represents a local extremum (trap). (b) The case $r_y^- r_y^+ < 0$: The equatorial singular arc $r^- \to r^+$ (thick orange line) is suboptimal relative to the bang-singular extremal $r^- \to r' \to r^+$ (thin black line).

$\frac{\pi}{2}\cos\alpha \leq \Delta\tau \leq \pi\cos\alpha$ for the case of time-optimal problem with constraint (4).

Consider now the extremals of type II. Let $\tau \in (\tilde{\tau}_{j-1}, \tilde{\tau}_j)$ be the singular arc where the relations (14b) hold. If $\tilde{\tau}_j \neq \tilde{T}$ when the time instant $\tau = \tilde{\tau}_j$ corresponds to the corner point between regular and singular arc. Suppose that there exists another corner point at $\tau = \tau_{j+1} > \tau_j$. Then it follows from eqs. (21) (19) and (17) that $\tilde{\Delta\tau}_j = \pi\cos\alpha$ and $U_{\tilde{\tau}_{j+1}, \tilde{\tau}_j} = -\hat{I}$, so that $\tilde{\rho}(\tilde{\tau}_{j+1}) = \tilde{\rho}(\tilde{\tau}_j)$. Using similar arguments, it is straightforward to derive the analogous result for possible corner points prior to τ_j. Thus, taking any 3-segment "anzatz" extremal similar to that shown in Fig. 1b, one can construct an infinite family $\mathcal{F}^{[\mathrm{k}]}(\tilde{u}(\tau))$ of $\mathrm{II}^{[\mathrm{k}]}$ extremals ($\mathrm{k} = k_1, k_2$) by randomly inserting k_1 and k_2 bang segments of length $\pi\cos\alpha$ with $u = +u_{\max}$ and $u = -u_{\max}$ into corner points of $\tilde{u}(\tau)$ or inside its singular arcs. It is clear that each family $\mathcal{F}^{[\mathrm{k}]}(\tilde{u}(\tau))$ constitutes the connected set of solutions, and all the members have equal performances J. Thus, the properties of any type II extremal can be reduced to the analysis of the equivalent three-segment ${}^0\mathrm{II}$ type or ${}^1\mathrm{II}$ type extremal, where all the positive and negative bang segments are merged into distinct continuous arcs separated by a singular arc.

The presented first-order analysis outlines the admissible profiles for optimal non-kinematic solutions (see Fig. 1). Moreover, by continuity argument (i.e. by considering the series of solutions with fixed $T \to T_{\mathrm{opt}}$ from below), these profiles should embrace all possible types of the stationary points of the time-optimal problem (2),(4). It is worth stressing that the latter include the globally optimal and everywhere singular kinematic solutions for which both segments with $u = \pm u_{\max}$ and $u = 0$ are singular. With this in mind, it is helpful to introduce the following terminological convention for the rest of the paper in order to avoid potential confusions: we will reserve the term "singular" exclusively for segments of extremals at which $u = 0$ whereas segments with $u = \pm u_{\max}$ will be always referred to as "bang" ones.

The reviewed results have several serious limitations. First, they do not allow to distinguish the globally time-optimal solution from a trap or a saddle point. Second, they do not provide *a priori* knowledge of the characteristic structural features of these stationary points (e.g. the expected type, number of switchings etc.) which is necessary to determine the topology of the landscape $J[u]$. These tasks require higher-order analysis, which is the subject of the next section.

III. DETAILED CHARACTERIZATION OF THE STATIONARY POINTS

In this section we will extensively use geometrical arguments in our reasoning. To make the presentation more visual, it is useful to expand the states and observables in the basis of Pauli matrices and identity matrix $\hat{I}$: $\rho = \frac{1}{2}\hat{I} + \sum_{i=x,y,z} r_i \hat{\sigma}_i$, $\hat{O} = \frac{1}{2}\,\mathrm{Tr}[\hat{O}]\hat{I} + \sum_{i=x,y,z} o_i \hat{\sigma}_i$. The dynamics induced by eq. (1) corresponds to rotation of the 3-dimensional Bloch vector $\vec{r} = \{r_x, r_y, r_z\}$ about the axis $\vec{n}_u \propto \{1, 0, u\}$ (note that the angle between $\vec{n}_{\pm u_{\max}}$ and $\vec{n}_0$ is equal to α, see e.g. Fig. 2), and the optimization goal (2) is equivalent to the requirement to arrange the state vector $\vec{r}$ in parallel to $\vec{o}$. In what follows we will often refer to the quantum states ρ as the endpoints r of vectors $\vec{r}$. Hereafter we will also assume that both r and o are renormalized such that $|r| = |o| = 1$.

We start by taking a closer look at type II extremals and their singular arc(s) where $\tilde{u}(\tau) = 0$. According to criterion (14b), these arcs are always located at the equatorial plane $x = 0$. The following proposition indicates that such arcs may represent the time-optimal solution at any values of $u_{\max}$ (see Appendix B for proof):

Proposition 1. *The shortest type II singular trajectory connecting any two "equatorial" points* $\vec{r}^{\,-} = \{0, r_y^-, r_z^-\}$ *and* $\vec{r}^{\,+} = \{0, r_y^+, r_z^+\}$ *(see Fig. 2) will represent the (globally) time-optimal solution if* $r_y^- r_y^+ > 0$, $(r_z^+ - r_z^-) r_y^- > 0$ *and a saddle point otherwise.*

Since all ${}^s\mathrm{II}$ extremals can be reduced to the effective 3-segment anzatz shown in Fig. 1b (see the end of the

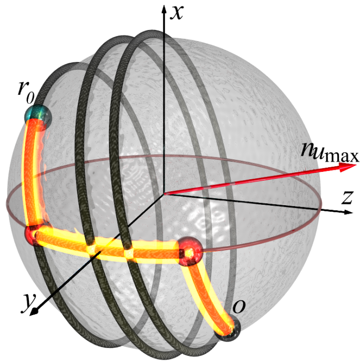

FIG. 3. The globally time-optimal ^{0}II type trajectory $\tilde{u}_{\rm anz}(\tau)$ (thick bright yellow curve) and the locally time-optimal trapping solution (black curve) of the $\mathcal{F}^{[3]}(\tilde{u}^{\rm anz}(\tau))$ family connecting the points $r_0{\propto}\{1,1,-1\}$ and $o{\propto}\{-1,1,1\}$.

previous section), Proposition 1 has the evident corollary:

Proposition 2. *All singular arcs of the locally optimal type II extremals are located in the same semi-space $y{>}0$ or $y{<}0$, and their total duration can not exceed $\pi/2$.*

For further analysis we need the following generic necessary condition for time optimality:

Proposition 3. *If the type I extremal $\{\tilde{u}(\tau),\tilde{r}(\tau)\}$ is locally time-optimal then each of its corner points $\tilde{r}_i$ satisfies the inequality*

$$\tilde{u}_i^{-}\,\tilde{r}_{i,x}\tilde{r}_{i,y}{\geq}0. \tag{22}$$

Qualitatively, Proposition 3 states that the projections of optimal trajectories on the xz-plane are always "V"-shaped at the corner points $\tilde{r}_i$ with $\tilde{r}_{i,x}{>}0$ and "Λ"-shaped otherwise (here we assume that the x-axis is oriented vertically, like in Fig. 2).

This result allows us to substantially narrow down the range of type II candidate trajectories:

Proposition 4. *Any type ^{s}II extremal with $s{>}0$ containing an interior bang arc is a saddle point for time-optimal control.*

In other words, all type ${}^{s}{\rm II}|_{s>0}$ locally time-optimal solutions reduce to the three-segment anzatz shown in Fig. 1b, where two regular arcs of duration $\tilde{\Delta}\tau_0,\tilde{\Delta}\tau_2{<}\pi\sec\alpha$ "wrap" the singular section where $u{=}0$. Accordingly, the number of control switchings is bounded by $n_{\rm II}{\leq}2$.

The properties of ^{0}II type extremals are richer:

Proposition 5. *Suppose that the ^{0}II type extremal $\tilde{u}(\tau)$ is the member of family $\mathcal{F}^{[k]}(\tilde{u}^{\rm anz}(\tau))$, and its anzatz $\tilde{u}^{\rm anz}(\tau)$ includes opening and closing bang segments of durations $\tilde{\Delta}\tau_0{>}0$ and $\tilde{\Delta}\tau_2{>}0$. Then $\tilde{u}(\tau)$ is locally optimal iif $\tilde{u}^{\rm anz}(\tau)$ is locally optimal.*

(for proof see Appendix E).

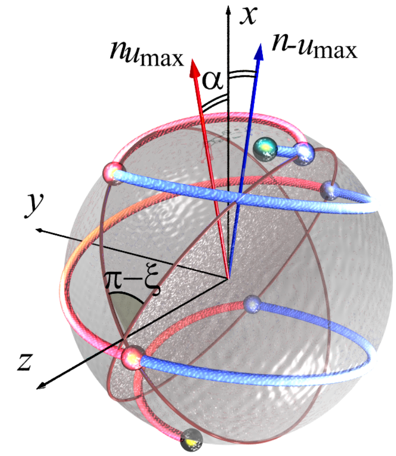

FIG. 4. Illustration of the statement of Proposition 6. The thick colored curve depicts the band-bang extremal. Its red and blue segments correspond to $u{=}{+}u_{\rm max}$ and $u{=}{-}u_{\rm max}$. All interior corner points (red and blue balls) lie on two circles (associated with switchings $u_{\rm max}{\to}{-}u_{\rm max}$ and ${-}u_{\rm max}{\to}u_{\rm max}$, respectively) whose planes $\lambda_{\pm1}$ intersect along the z-axis.

The analysis of type I extremals is somewhat more complicated. We begin by determining the loci of corner points $\tilde{r}_i$ on the Bloch sphere. Denote as $\theta{=}2\tilde{\Delta\tau}\sec\alpha$ the rotation angles on the Bloch sphere associated with the inner bang sections of the type I extremals. Note that it follows from (19), (20) that $\pi{<}\theta{<}2\pi$ in the case of a time-optimal control problem.

Proposition 6. *All the corner points $\tilde{r}_i$ of any locally optimal type I solution $\tilde{u}(\tau)$ of the problem (2), (3) are located on the circular intersections of the Bloch sphere with the two planes $\lambda_{\pm1}$ (see Fig. 4),*

$$\tilde{r}_i{=}\{{\rm sign}(\tilde{u}_i^{+})\sin(\gamma_i)\sin(\frac{\xi}{2}),-\sin(\gamma_i)\cos(\frac{\xi}{2}),\cos(\gamma_i)\}. \tag{23}$$

Here $\xi{=}{-}2\arctan\left(\frac{u_{\rm max}}{2}\tan(\frac{\theta}{2})\cos(\alpha)\right)$ is the dihedral angle between the planes $\lambda_{\pm1}$, and $\gamma_{i+1}{=}\gamma_1{+}i\eta$, where $\eta{=}{-}2\arctan\left(\frac{\sin(\frac{\theta}{2})}{\sqrt{u_{\rm max}^2{+}\cos^2(\frac{\theta}{2})}}\right)$.

Proposition 7. *Denote $q_i{=}q(\gamma_i){=}\cot^2(\gamma_i){-}\cot^2(\frac{\eta}{2})$ $(i{=}1,\dots,n)$. The set $\{q_i\}$ associated with any locally time-optimal extremal $\tilde{u}(t)$ contains at most one negative entry q', and $|q'|{=}\min(|\{q_i\}|)$.*

The proofs of the above two propositions are given in Appendix F.

To use Proposition 7, it is convenient to introduce parameters ζ_i through, $\zeta_1{=}\gamma_1{+}\frac{\pi}{2}(1{-}{\rm sign}(u_1^{+}))$, ζ_{i+1} = $\zeta_1{+}i(\pi{+}\eta)$. It is evident that $q(\gamma_i){=}q(\zeta_i)$. The relation between the sign of q_i and the index i of the corner point can be illustrated by associating each q_i with the point on the unit circle whose position is specified by ζ_i, as shown

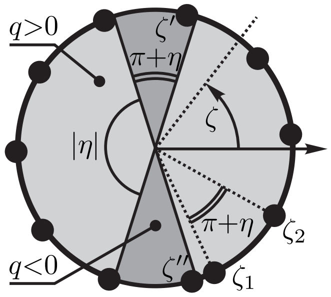

FIG. 5. Signs of the parameters $q(\zeta)$ as function of ζ. Black dots indicate the values $\zeta{=}\zeta_i$ associated with i-th corner point.

in Fig. 5. One can see that the maximal number $n_{\max}$ of sequential parameters q_i having at most one negative term can not exceed $\frac{\pi+|\eta|}{\pi-|\eta|}+1\le\frac{\pi}{\alpha}$, i.e.,

Proposition 8. *Type I locally optimal extremals can have at most* $\frac{\pi}{\alpha}$ *switchings.*

This helpful upper bound was first obtained by Agrachev and Gamkrelidze [27]. As shown in Appendix G, we can further refine this result via more detailed inspection of the criterion $|q'|{=}\min(|\{q_i\}|)$ as follows:

Proposition 9. $n_{\mathrm{I},\max}\le 2$ *if* $u_{\max}>\sqrt{1+\sqrt{2}}$

(The latter roughly corresponds to $\alpha{>}1$).

The analysis in this section so far is equally valid for both global and local extrema of optimal control. It is clear that any globally time-optimal type II solution includes at most 2 corner points that separate the central singular section from the outside regular arcs (see Fig. 1b). The case of type I solutions is not as evident. The following propositions impose more stringent necessary criteria on the globally time-optimal extremals (see Appendices H and I for proofs).

Proposition 10. *Any corner point* $\tilde{r}_{i'}$ *such that* $q(\gamma_{i'}){<}0$ *must be either the first or the last corner point of the globally time optimal solution, so that the total number of switchings* $n_{\mathrm{I},\max}\le\frac{\pi}{2\alpha}+1$.

Proposition 11. *The corner points* $\tilde{r}_i$ *of any globally optimal solution of type I satisfy the inequality*

$$\min(0,\tilde{r}_{0,x},\tilde{r}_{n+1,x})<\tilde{r}_{i,x}<\max(0,\tilde{r}_{0,x},\tilde{r}_{n+1,x}),\qquad(24)$$

where $\tilde{r}_{0,x}$ *and* $\tilde{r}_{n+1,x}$ *are the trajectory endpoints.*

Proposition 11 can be used to establish the following, more accurate, upper bound on the number of switchings (see Appendix J for proof).

Proposition 12. *The number of corner points of the globally time-optimal type I solution* $\tilde{u}(\tau)$ *is bounded by the following inequalities:*

$$n_{\mathrm{I}}\le\begin{cases}\max\left(\dfrac{\arccos(\frac{\tilde{r}_x^-}{\tilde{r}_x^+})}{|2\arctan(\frac{u_{\max}}{\tilde{r}_x^+})|},\dfrac{\pi}{|2\arctan(\frac{u_{\max}}{\tilde{r}_x^-})|}\right)+1 & \text{if } \tilde{r}_x^-\tilde{r}_x^+<0; \qquad (25a)\\[2ex] \min\left(\dfrac{\arccos(\frac{\tilde{r}_x^-}{\tilde{r}_x^+})}{|2\arctan(\frac{u_{\max}}{\tilde{r}_x^+})|}+3,\dfrac{\pi}{|4\arctan(\frac{u_{\max}}{\tilde{r}_x^+})|}\right)+1 & \text{if } \tilde{r}_x^-\tilde{r}_x^+>0, \qquad (25b)\end{cases}$$

where $\tilde{r}^+$ *and* $\tilde{r}^-$ *are new notations for the trajectory endpoints* $\tilde{r}_0$ *and* $\tilde{r}_{n+1}$, *such that* $|\tilde{r}_x^+|\ge|\tilde{r}_x^-|$.

Denote $\phi_\xi{=}|\theta_{r_0,\xi}{-}\theta_{o,\xi}|$ $(\xi = x,z)$, where $\theta_{r,\xi}$ is the angle between the axes $\vec{\epsilon}_\xi$ and $\vec{r}$. One can geometrically show that the maximum possible change $\Delta\theta_{r,\xi}^{\max}$ in $\theta_{r,\xi}$ generated by rotation about any of the axes $\vec{n}_{\pm u_{\max}}$ is $\Delta\theta_{r,x}^{\max}{=}2\alpha$ and $\Delta\theta_{r,z}^{\max}{=}\pi{-}2\alpha$ (see Fig. 6). This result allows us to establish the following lower bounds on the number of corner points:

Proposition 13. *The minimum number of corner points in locally time-optimal solutions reaching the global maximum of* J *is bounded by the inequalities*

$$n\ge\frac{|\arcsin(r_{0,x}){-}\arcsin(o_x)|}{2\arctan(u_{\max})}-1;\qquad(26a)$$

$$n_{\mathrm{I}}\ge\frac{|\arcsin(r_{0,z}){-}\arcsin(o_z)|}{2\mathrm{arccot}(u_{\max})}-1.\qquad(26b)$$

It is worth stressing that the bound (26b) is valid only for type I solutions.

Combination of the upper bounds on n imposed by Propositions 4 and 10 with inequalities (26) leads to the following conclusion:

Proposition 14. *The globally time-optimal solution(s) of problem* (2) *is of type I if*

$$\phi_x{=}\left|\arcsin(r_{0,x}){-}\arcsin(o_x)\right|>4\alpha\qquad(27a)$$

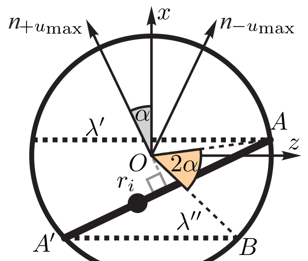

FIG. 6. Geometrical calculation of the value of $\Delta\theta_{r,x}^{\max}$. Rotation $\mathcal{S}_{\vec{n}_{-u_{\max}}}$ about vector $\vec{n}_{-u_{\max}}$ transfers any point r_i on the Bloch sphere into a new point on the AA' plane. The x-coordinate of this new point is bounded by the planes λ' and λ''. Thus, the associated change in $\theta_{r,x}$ is less than $\angle AOB{=}2\alpha$.

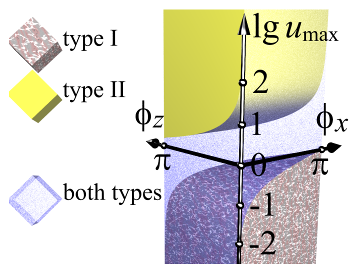

FIG. 7. Distribution of types of globally optimal solutions according to Proposition 14. Note that the admissible values of ϕ_x and ϕ_z are restricted by inequality $\phi_x{+}\phi_z{\leq}\pi$.

and of type II if

$$\phi_z{=}\,|\arcsin(r_{0,z}){-}\arcsin(o_z)|>\left[\frac{\pi}{2\alpha}{+}2\right](\pi{-}2\alpha). \quad (27b)$$

Note that this estimate can be further refined if combined with the upper bounds stated in Proposition 12. The statement of Proposition 14 is illustrated graphically in Fig. 7 which clearly shows that type I and type II solutions dominate in the opposite limits of tight and loose control restriction $u_{\max}{\to}0$ and $u_{\max}{\to}\infty$, respectively. Neither type, however, completely suppresses the other one at any finite positive value of $u_{\max}$. This coexistence sets the origin for the generic structure of suboptimal solutions (traps), whose analysis will be the subject of next two sections.

IV. TRAPS IN TIME-OPTIMAL CONTROL

The globally time-optimal solution (hereafter denoted as $\tilde{u}^{\rm opt}$) of the problem (2) can be supplemented by a number of trapping suboptimal solutions $\tilde{u}$ (characterized by $\tilde{J}{<}\tilde{J}^{\rm opt}$ and/or $\tilde{T}{>}\tilde{T}^{\rm opt}$) that are, however, optimal with respect to any infinitesimal variation of $\tilde{u}(\tau)$ and T. In particular, Proposition (2) implies that each locally optimal solution of type ^{0}II gives rise to the infinite family of traps of the form shown in Fig. 3. In what follows, we will call such traps "perfect loops". Proposition 1 indicates that perfect loops may exist at any value of $u_{\max}$. Nevertheless, their presence does not stipulate sufficient additional complications in finding the globally optimal solution by gradient search methods. Indeed, these "simple" traps can be identified at no cost by the presence of the continuous bang arc of the duration $\tilde{\Delta\tau_i}{\geq}\pi\sec(\alpha)$. Moreover, one can easily escape any such trap by inverting the sign of the control $u(\tau)$ at any continuous subsegment of this arc of duration $\pi\sec(\alpha)$ or by removing the respective time interval from the control policy.

For this reason, the primary objective of this section is to investigate the other, "less simple" types of traps which can be represented by type I and ^{s}II$|_{s>0}$ suboptimal extremals. Propositions 8, 10, 12, and 13 show that the number of switchings n in such extremals is always bounded (at least by π/α). Thus, the maximal number of such traps is also finite and decreases with increasing $u_{\max}$. It will be convenient to loosely classify the traps into the "deadlock", "loop" and "topological" ones as follows. The first two kinds of traps are represented by type I extremals. The deadlock traps are defined by inequalities $\tilde{J}{<}\tilde{J}^{\rm opt}$ $\tilde{T}{<}\tilde{T}^{\rm opt}$. They usually also satisfy the inequalities $n{<}n^{\rm opt}$. Their existence is mainly related to the fact that the distance to the destination point o for most extremals non-monotonically changes with time. The trajectory of the loop trap has the intersection with itself other than the perfect loop. These solutions require longer times $\tilde{T}{>}\tilde{T}^{\rm opt}$ and typically also larger numbers of switchings $n{>}n^{\rm opt}$ in order to reach the kinematic extremum $\tilde{J}{=}\tilde{J}^{\rm opt}$. Finally, the topological traps are associated with extremals of the type distinct from the type of the globally optimal solution. Of course, real traps can combine the features of all these three kinds.

Examples of the deadlock and loop traps are shown in Fig 8. In this case the globally time optimal solution with $n^{\rm opt}{=}4$ is accompanied by two deadlock traps and two degenerate loop traps corresponding to $n{=}5$ (only one is shown; the remaining solution can be obtained via subsequent reflections of the black trajectory relative to the yz and xy-planes). At the same time, no traps exist for $n{=}1,3$ and $n{>}5$.

The bang-bang extremal represented by blue curve $r^-{\to}r''{\to}r^+$ in Fig. 2a provides another example of the loop trap that is also the topological trap relative to type II optimal trajectory $r^-{\to}r^+$ (the specific parameters used in this example are: $u_{\max}{=}\frac{1}{2}$, $r^-{=}r_0{\propto}\{0,1,-\frac{1}{2}\}$, $r^+{=}o{\propto}\{0,1,1\}$). In general, once the endpoints r^- and r^+ satisfy the conditions of Proposition 1, the time-optimal solution remains the same type II trajectory even in the limit $u_{\max}{\to}0$, where the time optimal trajectories are mostly of type I (see Proposition 14 and Fig. 7). Moreover the traps of the shown form will exist for any value of $u_{\max}{<}\sqrt{4{-}(r_z^-{+}r_z^+)^2}/|r_z^- - r_z^+|$.

Another generic example of the traps of all three types can be straightforwardly constructed in the case $u_{\max}{\gg}1$ (see Fig. 9) by selecting $o{\propto}\{1,0,u_{\max}\}$ and choosing the

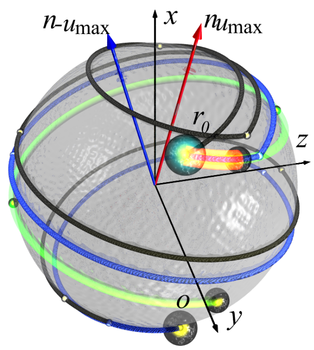

FIG. 8. Globally optimal solution (blue line), deadlock traps (light-red and green lines) and loop trap (black line) for the time-optimal control problem (2),(3),(4) with $u_{\max}=\frac{1}{4}$, $r(0)=\{\frac{1}{\sqrt{2}},\frac{1}{\sqrt{2}},0\}$, (big emerald dot) and $o=\{\frac{1}{\sqrt{2}},-\frac{1}{\sqrt{2}},0\}$ (big black-yellow dot). Small dots indicate the positions of corner points. The parameters of extremals are listed in the table:

extremal	sign($\tilde{u}_1^-$)	n	$\tilde{\Delta\tau}_1$	$\tilde{\Delta\tau}$	$\tilde{\Delta\tau}_{n+1}$
red	+	0	0.23	-	-
green	−	2	0.88	1.52	0.88
blue	+	4	0.33	1.78	0.33
black	−	5	1.15	1.72	0.57

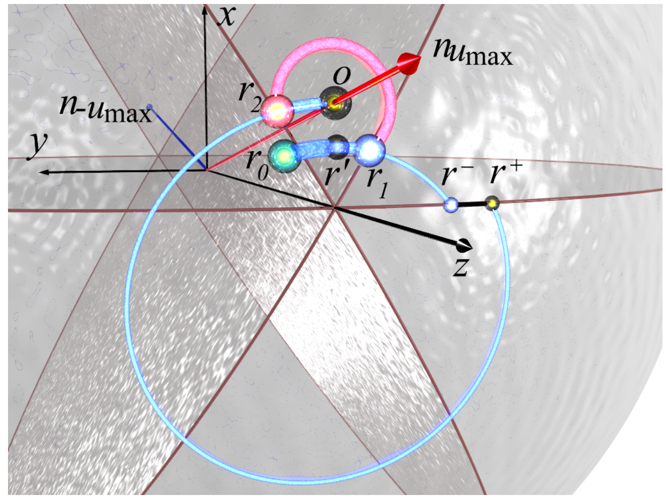

FIG. 9. The optimal solution (medium-thick trajectory $r_0\to r_1\to r_2\to o$), topological trap (thin trajectory $r_0\to r^-\to r^+\to o$) and deadlock trap (thick trajectory $r_0\to r'$) for the time-optimal control problem (2),(3),(4) with $u_{\max}=8$, $r(0)\propto\{\frac{1}{2},\frac{1}{2},u_{\max}\}$, $o\propto\{1,0,u_{\max}\}$. The segments colored blue\black\red correspond to $u(\tau)=-u_{\max}\backslash 0\backslash +u_{\max}$ and are associated with rotations about the axes $\vec{n}_{-u_{\max}}\backslash\vec{\epsilon}_x\backslash\vec{n}_{-u_{\max}}$. The durations $\Delta\tau_i$ of the consequent bang arcs are summarized in the table:

extremal	type	n	$\tilde{\Delta\tau}_1$	$\tilde{\Delta\tau}_2$	$\tilde{\Delta\tau}_3$
deadlock trap	I	0	0.020	-	-
optimal solution	I	2	0.0327	0.262	0.017
topological trap	II	2	0.075	0.031	0.324

initial state in vicinity of $z{=}1$: $r_0\propto\{c_1,c_2,u_{\max}\}$, where $0{<}c_1{<}1$ and c_2 is any sufficiently small number. Although the vast majority of time-optimal solutions are of type II in the limit $u_{\max}\to\infty$ (see Proposition 14), for this special choice the optimal solution is of type I for any finite value of $u_{\max}$ whereas the complementary type II extremal represents the topological trap. In the case $c_2{<}0$, there also exist a deadlock trap structurally similar to the ones shown in Fig. 8.

These observations lead to the following key proposition:

Proposition 15. *For any value of* $u_{\max}$ *there exist initial states* ρ_0 *and observables* $\hat{O}$*, such that the time optimal control problem* (2),(3) *has locally time-optimal solutions* $\tilde{u}(\tau)$ *representing non-simple traps.*

V. TRAPS IN FIXED-TIME OPTIMAL CONTROL

Consider the problem (2), (3) where the control time T is fixed. Specifically, we will be interested in the case

$$T{=}\mathrm{const}\gg\frac{\pi^2}{\alpha} \tag{28}$$

when the kinematically optimal solutions exist for any given ρ_0 and $\hat{O}$. We again will exclude the class of perfect loop traps from the analysis for the same reasons as in the previous section. Intuitively one can expect that the probability of trapping in the local extrema (other than perfect loops) should be small at large T. However, it is not clear if there exists such value of T that the functional (2) will become completely free of such traps.

To answer this question, note that in line with the analysis given in Sec. II any trap should be represented by either type I or type II extremal. However, the maximal number of switchings is not limited by inequalities similar to Proposition 8. At the same time, Proposition 6 remains applicable (see *Remark 1* in Appendix F). Recall that its proof is based on introduction of the "sliding" variations $\delta\gamma_i$ which shift the angular positions of the "images" of corner points on the diagram of Fig. 5 (see Appendix F). The explicit expression for the "sliding" variation around the i-th corner point up to the third order in the associated control time change $\delta\tau_i$ is given by eq. (F4). By definition, if the trajectory $\tilde{u}(\tau)$ is type I trap, then no admissible control variation δu can improve the performance index (2). Consider the subset Ω of such variations composed of infinitesimal sliding variations $\delta\gamma_i$ that preserve the total control time T. Then, the necessary condition of trap $\tilde{u}(\tau)$ is absence of the non-uniform sliding variation $\delta u(\tau)\in\Omega$ that leaves the trajectory endpoint r_{n+1} intact. Indeed, the trajectory associated with varied control $\tilde{u}{+}\delta u$ would deliver the same value of the performance index but at the same time is not the locally optimal solution (since it is no longer the type I extremal) which implies that $\tilde{u}$ is not locally optimal.

Using (F4) the stated necessary condition can be rewritten as the requirement of definite signature of the quadratic form (F6), where the parameters q_i were introduced in Proposition (7). The necessary condition of the sign definiteness is that all (probably except one) parameters q_i are either non-positive or non-negative. Using Fig. 5 one can see that in the case of long T only the second option can be realized with $\eta{\simeq}0$, $\eta{\simeq}-\frac{\pi}{2}$ and $\eta{\simeq}-\frac{\pi}{3}$ (the case $\eta{\simeq}-\pi$ must be eliminated because it implies $u_{\max}{=}0$). One can show that the last two variants lead to saddle points rather that to the local extrema. The remaining case $\eta{\simeq}0$ leaves the two options $\theta{\simeq}0$ and $\theta{\simeq}2\pi$. The last option corresponds to positive constant $c_{i,1}$ in (15), which indicates the possibility of increasing J via monotonic "stretching" the time: $T{\to}T{+}\delta T(T)$, $u(\tau){\to}u(\tau{-}\delta T(\tau))$, where $\delta T(\tau)$ is an infinitesimal positive monotonically increasing function. At the same time, the associated parameters q_i are all negative, so there exists the combination of variations $\delta\tau$ of arcs durations $\Delta\tau$ which will result in achieving the same value of the performance index at shorter time. Thus, we can conclude that it is also possible to increase J at fixed time T via proper combination of these two variations, so the variant $\theta{\simeq}2\pi$ should be dismissed as a saddle point. Only the remaining choice $\theta{\simeq}0$ is consistent with an arbitrary number of q_i of the same sign. However, in this case the length of each bang arc also reduces to zero. As result, the maximal duration of such optimal trajectories is limited by the inequality $T{\lesssim}\pi$.

This analysis leads us to remarkable conclusion:

Proposition 16. *The fixed-time optimal control problem* (2) *is free of non-simple traps for sufficiently long control times T.*

The spirit of this conclusion is in line with the results of numerical simulations performed in [19]. With this, it is worth recalling that the general time-fixed problem may have a variety of perfect loop traps for any value of $u_{\max}$ and, thus, is not trap-free in the strict sense. These traps were missed in the simulations in [19] due to the specifics of numerical optimization procedure.

VI. SUMMARY AND CONCLUSION

All stationary points of the time optimal control problem and all saddles and local extrema of the fixed-time optimal control problem are represented by the piecewise-constant controls of types I and II sketched in Fig. 1 (the associated characteristic trajectories $\rho(\tau)$ on the Bloch sphere are shown in Figs. 4 and 3, correspondingly). We systematically explored the anatomy of stationary points of each type. Specifically, we identified the locations and relative arrangements of corner points on the Bloch sphere (propositions 2, 3, 6, 7, 10, 11) and estimated their total number (propositions 8, 9, 10, 12, 13). These characteristics, together with propositions 1, 4, 5 and 14, allow to determine whether the given extremal is a saddle point or a locally optimal solution, and also to predict the shape of globally optimal solution. The presented results (except Proposition 8) substantially generalize and refine the estimates obtained in previous studies [25, 26]. Moreover, this study, to our knowledge, is the first example of a systematic analytic exploration of the overall topology of the quantum landscape $J[u]$ in the presence of constraints on the control u and for the arbitrary initial quantum state ρ_0 and observable $\hat{O}$. In particular, we distinguished 4 categories of traps tentatively called deadlock, topological, loop and perfect loop traps. The landscape can contain an infinite number of perfect loops whereas the number of traps of other types is always finite. Among them, the number of deadlock traps and loops decreases with increasing value of the constraint $u_{\max}$ in eq. (4). Nevertheless, we have shown by an explicit example that the traps of all categories can simultaneously complicate the landscape $J[u]$ of the time-optimal control problem regardless of the value of $u_{\max}$. So, this is the case where the intuitive attempt to "extrapolate" the conclusions based on analysis of the case of unconstrained controls totally fails.

The fixed-time control problem is more intriguing. On one hand we formally showed that it is impossible to completely eliminate all the traps in this case by increasing the value of $u_{\max}$. This result is in line with generic experience concerning the optimal control in technical applications. However, if the control time is long enough (specifically, if $T{\gg}\pi^2/\arctan u_{\max}$) the only traps which can survive are perfect loops. Remarkably, these traps can be easily avoided at virtually no computational cost.

Combined together, our results constitute a thorough guide for optimal control synthesis to manipulate the individual qubit in a variety of experiments with cold atoms, Bose-Einstein condensates, superconducting qubits etc. However, they also deliver more general message since the stable control over single-qubit operations is the necessary controllability prerequisite for a variety of quantum control problems including the universal quantum information processing. We can conclude that traps constitute a general obstacle for practical optimization, and their presence can not be ignored. Nevertheless, we have demonstrated that there can exist simple "patches" to standard gradient search algorithms such that the quantum landscape will appear as trap-free from practical perspective. The latter conclusion is consistent with the common viewpoint in the quantum optimal control literature. That said, validity of the same conclusion in the general case remains an open question.

The key methodological feature of the presented derivations is introduction of the sliding variations, which makes it possible to extensively rely on highly visual and intuitive geometrical arguments. For this reason, we believe that the mathematical aspect of the paper constitutes instructive introduction into high-order analysis of optimal processes.

Appendix A: Review of the Pontryagin maximum principle

In this appendix we briefly overview the concepts of the Pontryagin theory and outline the derivations of the key statements and relations of Sec. II. Consider the following canonical optimal control problem [10, 11]:

$$\frac{\partial}{\partial t}\, x_i{=}f_i(\mathbf{x},\mathbf{u},t) \quad (i{=}1,...,n); \tag{A1a}$$
$$g_j(\mathbf{x}(t_0),\mathbf{x}(T),t_0,T){=}0 \quad (j{=}1,...,q{<}2n{+}2); \tag{A1b}$$
$$\mathbf{u}{\in}\mathcal{U}; \tag{A1c}$$
$$J{\to}\max\,. \tag{A1d}$$

Here $\mathbf{x}{=}\{x_1,...,x_n\}$ and $\mathbf{u}{=}\{u_1,...,u_m\}$ are the vectors of phase variables and the available controls, correspondingly. The functions g_j introduce the boundary constraints on the admissible values of $\mathbf{x}$ whereas eq. (A1c) describes the control constrains, which are the generalization of eq. (3). The most general (Bolza) form of the performance index J in (A1d) is

$$J{=}g_0(\mathbf{x}(t_0),\mathbf{x}(T),t_0,T){+}\int_{t_0}^{T} f_0(\mathbf{x},\mathbf{u},t)dt. \tag{A1e}$$

The task is to find the control policy $\tilde{u}(t)$ and, maybe, the final time T together with the initial and terminal phase variables $\mathbf{x}(t_0)$ and $\mathbf{x}(T)$ which maximize J.

Let us introduce the following auxiliary functions:

$$K{=}\sum_{i=0}^{N}\Psi_i f_i \qquad \text{— Pontryagin function;} \tag{A2}$$
$$G{=}\sum_{j=0}^{q}\nu_j g_j \qquad \text{— terminant,} \tag{A3}$$

where $\nu_0,\Psi_0{=}\,\mathrm{const}\geq 0$ and the $\Psi(t)$ stands for the set of so-called *costate* (or *adjoint*) variables. By definition,

$$\frac{\partial}{\partial t}\, x_i{=}\frac{\partial K}{\partial \Psi_i} \qquad (\textit{cf.}\ \text{(A1a)}); \tag{A4a}$$
$$\frac{\partial}{\partial t}\,\Psi_i{=}{-}\,\frac{\partial K}{\partial x_i}\,. \tag{A4b}$$

Mathematically, the functions $\Psi_i(t)$ and variables ν_j are the Lagrange multipliers in the extremal problem (A1d) that account for the dynamic and boundary constraints (A1a) and (A1b), respectively. The process (trajectory) $\{\Psi(t),\mathbf{u}(t),\mathbf{x}(t)\}$ is called *admissible* if it matches eqs. (A4) and the boundary conditions (A1b).

The *Pontryagin maximum principle* (PMP) states that if $\{\tilde{\mathbf{x}}(t),\tilde{\Psi}(t),\tilde{\mathbf{u}}(t)\}$ is an (locally) optimal solution of problem (A1) then $\tilde{\Psi}_0{\geq}0$, $\tilde{\Psi}(t){\neq}0$ and

$$\tilde{\mathbf{u}}(t){=}\arg\max_{\mathbf{u}(t)\in\mathcal{U}} K(\tilde{\mathbf{x}}(t),\tilde{\Psi}(t),\mathbf{u}(t),t). \tag{A5}$$

Besides that, the following *transversality conditions* hold:

$$\tilde{\Psi}_i(t_0){=}{-}\,\frac{\partial G}{\partial x_i(t_0)}; \qquad \tilde{\Psi}_i(T){=}\,\frac{\partial G}{\partial x_i(T)}; \tag{A6}$$
$$\tilde{K}\Big|_{t=t_0}{=}\,\frac{\partial G}{\partial t_0}; \qquad \tilde{K}\Big|_{t=T}{=}{-}\,\frac{\partial G}{\partial T}\,. \tag{A7}$$

Processes satisfying (A5)-(A7) are called *extremals.* Any solution of the problem (A1) is extremal. The reverse is not true since PMP provides only the first-order necessary optimality condition. To identify the solutions, the Legendre-Clebsch condition and its generalizations [32], or other higher-order extensions of PMP should be used [31].

In the general case, the optimal controls $\tilde{u}_k(t)$ are the piecewise-smooth curves composed of *regular* and *singular* (or *degenerate*) subarcs and having any number of discontinuities of the first kind (*corner points*). The values of $\tilde{u}_k(t)$ on regular subarcs can be directly obtained from (A5) whereas the singular subarcs where $\frac{\partial\tilde{K}}{\partial u_k}{=}0$ require an extra investigation. The following *Weierstrass-Erdmann conditions* must hold at each corner point:

$$\Psi|_{t-0}=\Psi|_{t+0}\,; \qquad K|_{t-0}=K|_{t+0}\,. \tag{A8}$$

Let us now outline the application of PMP to the quantum optimal control problem (1)-(4). In this case, the state vector $\mathbf{x}(t)$ is composed of matrix elements of the density matrix $\rho(t)$ and the control $\mathbf{u}(t)$ reduces to a scalar function $u(t)$. The performance index (2) is a special case of (A1d), where $f_0{=}0$ (a so-called Mayer problem). Using the definition (A2), one straightforwardly obtains the expression (6) for a Pontryagin function, where the matrix elements of $\hat{O}(t)$ serve as the components of a costate vector $\Psi(t)$. Application of (A4b) to (6) gives the evolution law (7). The endpoint relation (8) stems from the second of the transversality conditions (A6) with $G{=}g_0(\rho(T)){=}Tr[\rho(T)\hat{O}]$, whereas the second pair of transversality conditions (A7) leads to the property (11). Finally, note that the Pontryagin function (6) does not explicitly depend on time t. Hence, eqs. (A4) imply the relation (10) since $\frac{d}{dt}\tilde{K}{=}\frac{\partial\tilde{K}}{\partial\rho}\frac{d\tilde{\rho}}{dt}+\frac{\partial\tilde{K}}{\partial\hat{\tilde{O}}}\frac{d\hat{\tilde{O}}}{dt}{=}0.$

Appendix B: Proof of Proposition 1

Here we consider the case $r_y^-{>}0,r_y^+{>}0$. The case $r_y^-{<}0,r_y^+{<}0$ can be treated similarly. Simple geometrical analysis leads to the following expression for the travel time difference δT between bang-bang (orange) and "equatorial" (black) trajectories shown in Fig. 2a:

$$\delta T_{\rm a}=\cos(\alpha)\left(\arcsin\left(\frac{\frac{\delta_z}{2}\sec(\alpha)-\cos(\alpha)r_z^+}{\sqrt{1-\sin^2(\alpha){r_z^+}^2}}\right)+\arcsin(\frac{\cos(\alpha)r_z^+}{\sqrt{1-\sin^2(\alpha){r_z^+}^2}})-\arcsin(\frac{\cos(\alpha)r_z^-}{\sqrt{1-\sin^2(\alpha){r_z^-}^2}})+\arcsin(\frac{\frac{\delta_z}{2}\sec(\alpha)+\cos(\alpha)r_z^-}{\sqrt{1-\sin^2(\alpha){r_z^-}^2}})\right)-\arcsin(r_z^+)+\arcsin(r_z^-), \tag{B1}$$

where $\delta_z{=}r_z^+-r_z^-$. Let us fix one of the endpoints $r^\pm$ and vary the position of another one. Note that $\delta T_{\rm a}|_{\delta_z=0}{=}0$ for any admissible value of $r_z^\pm$. Furthermore,

$$\pm\frac{d\delta T_{\rm a}}{dr_z^\pm}=\frac{(1{-}{r_z^\pm}^2)\left(\sqrt{1{-}\frac{r_z^\pm\delta_z}{1-{r_z^\pm}^2}}-\sqrt{1{-}\frac{r_z^\pm\delta_z+\frac{\delta_z^2}{4}\sec^2\alpha}{1-{r_z^\pm}^2}}\right)}{\left(\csc^2\alpha{-}{r_z^\pm}^2\right)\sqrt{1{-}r_z^\pm\delta_z{-}{r_z^\pm}^2{-}\frac{\delta_z^2}{4}\sec^2\alpha}}>0. \tag{B2}$$

This allows to conclude that $\delta T_{\rm a}{>}0$ for any $\delta_z{>}0$ which finishes the proof of Proposition for the case $r_y^-r_y^+{>}0$.

Consider now the case $r_y^-r_y^+{<}0$. For clarity, we will assume that $r_y^-{>}0$ $r_z^-{<}r_z^+$ (see Fig. 2b). The remaining cases can be analyzed similarly. The time difference $\delta T_{\rm b}$ between "equatorial" (black) and the green trajectories and its derivative with respect to the position of the endpoint r_z^+ read as

$$\delta T_{\rm b}{=}\arccos(r_z^+){-}\cos(\alpha)\arccos\left(\frac{r_z^+\cos(\alpha)}{\sqrt{1-{r_z^+}^2\sin^2(\alpha)}}\right); \tag{B3}$$

$$\frac{\partial}{\partial r_z^+}\,\delta T_{\rm b}{=}{-}\frac{2\sqrt{1{-}{r_z^+}^2}\sin^2(\alpha)}{{r_z^+}^2\cos(2\alpha){-}{r_z^+}^2{+}2}. \tag{B4}$$

These expressions show that $\delta T_{\rm b}|_{r_z^+=1}{=}0$ and that $\frac{\partial}{\partial r_z^+}\,\delta T_{\rm b}{>}0$ for any admissible value of r_z^+. Thus, $\delta T_{\rm b}{>}0$ which proofs Proposition for the case $r_y^-r_y^+{<}0$.

Appendix C: Proof of Proposition 3

The proof is based on explicit construction of the second-order McShane's (needle) variation of the control $\tilde{u}(\tau)$ which decreases $\tilde{T}$ if the inequality (22) is violated. Choose arbitrary infinitesimal parameter $\delta\tau^-{\to}0$ and denote $r_i^-{=}\tilde{r}(\tilde{\tau}_i{-}\delta\tau^-)$. Under assumptions of Proposition it is always possible (except for the trivial case $\tilde{r}_{i,y}{=}0$) to choose another small parameter $\delta\tau^+$ such that the state vector $r_i^+{=}\tilde{r}(\tilde{\tau}_i{+}\delta\tau^+)$ obeys the equality: $r_{i,x}^-{=}r_{i,x}^+$. It is evident that the Bloch vector $r_{i,x}^-$ can also reach $r_{i,x}^+$ in the course of free evolution with $u{=}0$ after certain time $\delta\tau^0$. If we require that $\delta\tau_i^+,\delta\tau_i^0|_{\delta\tau_i^-\to 0}{=}0$ then both τ_i^+ and τ_i^0 are uniquely defined by $\delta\tau_i^-$,

$$\delta\tau_i^+{=}\frac{\delta\tau_i^-(\tilde{r}_{i,y}{+}2\delta\tau_i^-\tilde{r}_{i,z})}{\tilde{r}_{i,y}}+o({\delta\tau_i^-}^2);$$
$$\delta\tau_i^0{=}\frac{2\delta\tau_i^-(\delta\tau_i^-(\tilde{u}_i^-\tilde{r}_{i,x}{+}\tilde{r}_{i,z}){+}\tilde{r}_{i,y})}{\tilde{r}_{i,y}}, \tag{C1}$$

and thus, $\delta\tau_i^0{-}\delta\tau^+{-}\delta\tau^-{=}2\tilde{u}_i^-\left(\delta\tau_i^-\right)^2\tilde{r}_{i,x}/\tilde{r}_{i,y}$. The latter quantity should be nonnegative for the locally time-optimal solution which leads to eq. (22).

Appendix D: Proof of Proposition 4

Consider any type ^{s}II extremal with $s{>}0$ containing at least one interior bang segment $\tau{\in}[\tilde{\tau}_i,\tilde{\tau}_{i+1}]$ of length $\tilde{\Delta\tau}_i{=}m\pi\cos(\alpha)$ $(m{\in}\mathbb{N}, 0{<}\tilde{\tau}_i,\tilde{\tau}_{i+1}{<}T)$. Since $\tilde{r}_i{=}\tilde{r}_{i+1}$ both the value of the performance index J and duration T will not change if this segment will be "translated" in arbitrary new point $\tilde{r}(\tau_i'(\kappa))$ of extremal via the following continuous variation $\tilde{u}(\tau){\to}u(\kappa,\tau)$ $({-}\tau_i{<}\kappa{<}T{-}m\pi\cos\alpha)$:

$$u(\kappa,\tau){=}\begin{cases}\tilde{u}(\tau), & \tau{<}\tilde{\tau}_i{+}\frac{\kappa-|\kappa|}{2}\vee\tau{>}\tilde{\tau}_{i+1}{+}\frac{\kappa+|\kappa|}{2};\\ \tilde{u}_i^+, & \tilde{\tau}_i{+}\kappa{<}\tau{<}\tilde{\tau}_{i+1}{+}\kappa;\\ u(\tau{-}\tilde{\Delta\tau}_i) & \text{otherwise},\end{cases} \tag{D1}$$

where $\tau'(\kappa){=}\tilde{\tau}_i{+}\kappa{+}\frac{1}{2}(1{+}\frac{\kappa}{|\kappa|})\tilde{\Delta\tau}_i$.

Suppose that $\tilde{u}(\tau)$ is locally time-optimal solution. Then the entire family of control policies $\{u(\kappa,\tau),r(\kappa,\tau)\}$ should be locally time-optimal too. Since $s{>}0$ it is always possible to select the value $\kappa{=}\kappa_0$ such that $\tilde{r}(\tau'(\kappa_0))$ is interior point of the bang arc with $\tilde{u}(\tau'(\kappa_0)){=}{-}\tilde{u}_i^+$ and $\tilde{r}_x(\tau'(\kappa_0)){\neq}0$. However, the resulting trajectory $r(\kappa_0,\tau)$ is both Λ- and V-shaped in the neighborhood of point $r(\tilde{\tau}_i{+}\kappa_0){=}r(\tilde{\tau}_{i+1}{+}\kappa_0)$. According to Proposition (3) such trajectory can not be time-optimal. The obtained contradiction finishes the proof.

Appendix E: Proof of Proposition 5

Let $u'(\tau)$ be the control strategy obtained via arbitrary McShane variation $\delta u(\tau)$ of the control $\tilde{u}(\tau)$. Let us show that $u'(\tau)$ is less time efficient than some member $u''(\tau)$ of the control family $\mathcal{F}^{[\rm k]}({u''}^{\rm anz}(\tau))$ with the same k but perhaps the different anzatz $\tilde{u''}^{\rm anz}$. For this we will need the following lemma which is complementary to Propositions 1 and 3:

Lemma 1. *Suppose that $r'(\tau')$ is junction point of two bang arcs of the trajectory $u(\tau)$ such that $r_x'{=}0$. Consider*

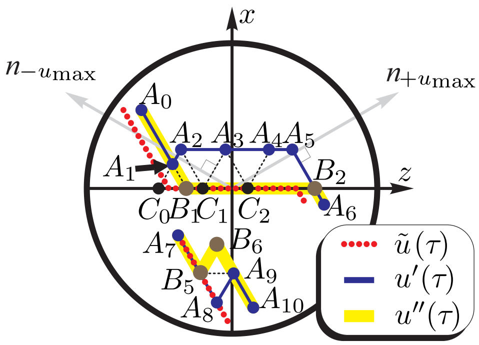

FIG. 10. Projections of the characteristic pieces of the original, varied and reduced trajectories $\tilde{r}(\tau)$, $r'(\tau)$ and $r''(\tau)$ on the xz plane (it is assumed that y-components of all shown parts of trajectories are greater than zero). The color associations are indicated in the inset.

any two points $r^-(\tau^-)$ and $r^+(\tau^+)$ $(\tau^-<\tau'<\tau^+)$ on adjacent arcs such that $r_x^-=r_x^+$ and the complete segment $r'_y r_y(\tau)>0$ for any $\tau\in(\tau^-,\tau^+)$. Denote as $\widehat{\Delta\tau}$ the minimal duration of free evolution (u=0) required to reach r^+ starting from r^-. Then, $\widehat{\Delta\tau}>\tau^+-\tau^-$.

Since $\tilde{u}_{\rm anz}(\tau)$ is locally optimal by assumption it is sufficient to consider the variations of the $\delta u(\tau)$ which do not involve the vicinities of the trajectory endpoints. Moreover, it is sufficient to analyze the variations $\delta u(\tau)$ which are nonzero only in vicinities points where $\tilde{r}(\tau)$=0. To show this consider the McShane variation in the arbitrary interior point A_8 of the bang arc (see Fig. 10). Consider the piece $A_7A_8A_9A_10$ of the varied trajectory $r'(\tau)$. According to Proposition 3 (see eq. (C)) the path $B_5B_6A_9$ is more time-efficient than $B_5A_8A_9$ if the varied segment A_8A_9 is sufficiently small. Thus, the trajectory $A_7B_5B_6A_10$ is more time-efficient than original segment $A_7A_8A_9A_10$. By repeated application of the same reasoning to the modified pieces of trajectory one can replace the control $u'(\tau)$ with the more effective strategy which differs from $\tilde{u}(\tau)$ only in vicinities of the points r' with $r'_x\to 0$. Since it is sufficient to consider only this modified control policy we will rename it as $u'(\tau)$ and will refer as the initial variation in the subsequent analysis.

The characteristic piece $A_0A_2A_5A_6$ of the resultant trajectory is shown in Fig. 10. Following the proof of Proposition 1 (see eq. (B2)) the path $C_0A_2C_1$ is less time-efficient than $C_0A_1B_1C_1$. This implies that the path $A_1B_1C_1$ is more time-efficient than $A_1A_2C_1$. According to Lemma 1, the path $A_2C_1A_3$ is more time-efficient than the path A_2A_3 associated with the free evolution. As a result, the trajectory segment $A_1A_2A_3$ of the $r'(\tau)$ is less time efficient than the combination of the segment $A_1B_1C_1$ of the trajectory $r''(\tau)$ with the segment C_1A_3. By continuing the similar analysis one finally comes to conclusion that the part of trajectory $r'(\tau)$ between the points A_0 and A_5 is less time efficient than the corresponding segment of $u''(\tau)$. Applying the same reasoning to the entire trajectory $r'(\tau)$ we will reduce the original variation to the ${}^0II$ type control $u''(\tau)$ and trajectory $r''(\tau)$. Note that we must assume that all the singular segments where $u''(\tau)$=0 are located on the same side with respect to xz plane (otherwise the control time can be further reduced by eliminating some singular segments following the proof of Proposition 2, see eq. (C)). This mean, that all the interior bang sections of the control $u''(\tau)$ are of length $m\pi/cos(\alpha)$ ($m\in\mathbb{N}$). Thus, the trajectory $u''(\tau)$=0 must belong to the family $\mathcal{F}^{[\rm k]}(u''^{\rm anz}(\tau))$ with the same index k as $\mathcal{F}^{[\rm k]}(u''^{\rm anz}(\tau))$ and the anzatz $u''^{\rm anz}(\tau)$ related to $\tilde{u}^{\rm anz}(\tau)$ via infinitesimal variation. Since $\tilde{u}^{\rm anz}(\tau)$ is time-optimal the performances and control times associated with policies $u''^{\rm anz}$ and $\tilde{u}^{\rm anz}$ are related as $\tilde{J}^{\rm anz}\geq J''^{\rm anz}$ and $\tilde{T}^{\rm anz}\leq T''^{\rm anz}$. Consequently, $\tilde{J}\geq J''$ and $\tilde{T}\leq T''$, so that the control policies $u''(\tau)$ and $u'(\tau)$ can not be more effective than $\tilde{u}(\tau)$. The latter conclusion completes the proof of Proposition 5.

Proof of the Lemma 1. For concreteness, consider the case $r'_y>0$, $r_x^->0$. Denote $\widehat{\delta\tau}=r^+(\tau^+)-r^+(\tau^+)-\widehat{\Delta\tau}$. Using simple geometrical considerations one can find that

$$\widehat{\delta\tau}(r_x^-,r'_z)=\frac{1}{2}\sum_{s=\pm1}\left(\arcsin\left(\frac{sr'_z-r_x^-\cot(\alpha)}{\sqrt{1-{r_x^-}^2}}\right)+\frac{\arcsin\left(\frac{r_x^-\csc(\alpha)-sr'_z\cos(\alpha)}{\sqrt{1-{r'_z}^2\sin^2(\alpha)}}\right)}{\sqrt{\tan^2(\alpha)+1}}\right). \tag{E1}$$

By differentiating (E1) we find that $\frac{\partial}{\partial r_x^-}\widehat{\delta\tau}(r_x^-,r'_z{=}0)=-\frac{x^2\sin(2\alpha)\sqrt{1-x^2\csc^2(\alpha)}}{(x^2-1)(\cos(2\alpha)+2x^2-1)}<0$ for any admissible $r_x^->0$. Similarly, one can show that $\widehat{\delta\tau}(r_x^-{=}0,r'_z)=0$ and $r'_z\frac{\partial}{\partial r'_z}\widehat{\delta\tau}(r_x^-,r'_z)<0$ for any admissible $r'_z\neq 0$. Taken together, these relations lead to conclusion that $\widehat{\delta\tau}(r_x^-,r'_z)<0$ for any admissible $r_x^->0$ which completes the proof for the case $r'_y>0$, $r_x^->0$. Other cases can be analyzed in the same way. □

Appendix F: Proof of Proposition 6 and 7

One can directly check that the transformation $\mathcal{S}_\pm=\exp(\tilde{\Delta\tau}\mathcal{L}(\pm u_{\max}))$ is equivalent to the composition of rotation $\mathcal{S}_{\vec{\epsilon}_z}(\mp\xi)$ around axis $\vec{\epsilon}_z$ by angle $\mp\xi$ with rotation $\mathcal{S}_{\vec{n}_{\pm u_{\max}}}(\eta)$ around the normal vector $\vec{n}_{\pm u_{\max}}$ to the plane $\lambda_{\pm u_{\max}}$ by η,

$$\mathcal{S}_\pm=\mathcal{S}_{\vec{n}_{\pm1}}(\eta)\mathcal{S}_{\vec{\epsilon}_z}(\mp\xi)\quad(-\pi<\eta<0;\quad 0<\xi<\pi), \tag{F1}$$

where the domain restrictions on the values of η and ξ result from (19). Thus, the state transformation induced by any two subsequent bang arcs is equivalent to rotation around $\vec{n}_{\pm u_{\max}}$ by angle 2η. This proofs that the all odd (even) corner points are located in the same plane orthogonal to $\vec{n}_{u_1^-}$ $(\vec{n}_{u_1^+})$ and parallel to $\vec{\epsilon}_z$. More specifically, they are located on the circles $\vec{r}\vec{n}_{\pm u_{\max}}=c_0$ which are mirror images of each other in xz plane.

In order to complete proof of Proposition 6 it remains to show that $\vec{\epsilon}_z \in \lambda_{\pm u_{\max}}$ (i.e. that $c_0=0$). Since it is already shown that $\vec{\epsilon}_z \| \lambda_{\pm u_{\max}}$ it is enough to prove that there exist an least one common point with axis $\vec{\epsilon}_z$. Consider the infinitesimal variations $\delta\tau_i^-$ and $\delta\tau_i^+$ of the durations $\tilde{\Delta\tau}_i$ and $\tilde{\Delta\tau}_{i+1}$ of the bang arcs adjacent to arbitrary corner point $\tilde{r}_i = \tilde{r}(\tilde{\tau}_i)$, such that the transformation $\mathcal{S} = \exp(\delta\tau_i^- \mathcal{L}(\tilde{u}_i^-)) \exp(\delta\tau_i^+ \mathcal{L}(\tilde{u}_i^+))$ moves the point $\tilde{r}_i$ into $r_i' \in \lambda_{\tilde{u}_i^-}$. In other words, we require that $\tilde{r}_i$ and r_i' should relate by infinitesimal rotation $\mathcal{S}_{\vec{n}_{\tilde{u}_i^-}}(\delta\gamma_i)$. For convenience, we will call such variations as "sliding" ones. The form of decomposition (F1) indicates that the sliding variation at r_i shifts the locations of all subsequent corner points $\tilde{r}_{j>i} \to r_j'$ by similar rotations $\mathcal{S}_{\vec{n}_{u_j^-}}(\delta\gamma_i)$ around the associated axes $\vec{n}_{u_j^-}$. Consider the arbitrary composition of the sliding variations, such that the trajectory start and end points remain fixed, i.e. $\sum_i \delta\gamma_i = 0$. If the extremal $\tilde{u}$ is locally optimal then such variations should not allow the reduction of the control time T: $\sum_i \delta\tau_i \leq 0$, where $\delta\tau_i = \delta\tau_i^- + \delta\tau_i^+$. This requirement leads to the following first-order (in $\delta\tau_i$) necessary optimality condition:

$$\forall i, j : \frac{d\delta\gamma_i}{d\delta\tau_i} = \frac{d\delta\gamma_j}{d\delta\tau_j} \,. \tag{F2}$$

Using simple geometrical analysis it is possible to explicitly calculate the derivatives in (F2),

$$\frac{d\delta\gamma_i}{d\delta\tau_i} = \frac{2\sqrt{\cos^2\left(\frac{\theta}{2}\right) + u_{\max}^2}}{\frac{\tilde{r}_{i,x}}{\tilde{r}_{i,y}} \tilde{u}_i^- \sin\left(\frac{\theta}{2}\right) - \sqrt{1+u_{\max}^2} \cos\left(\frac{\theta}{2}\right)} . \tag{F3}$$

We can conclude that equalities (F2) are equivalent to condition: $\frac{\tilde{r}_{i,x}}{\tilde{r}_{i,y}} \tilde{u}_i^- = \text{const}$ which directly leads to conclusion that $\vec{\epsilon}_z \in \lambda_{\pm 1}$ and completes the proof of Proposition 6.

Remark 1. It is worth stressing that the above proof of Proposition 6 does not explicitly depend on the time optimality of the trajectory $\tilde{u}(\tau)$. Thus, its statement is generally valid for any type I extremal locally optimal with respect to small variations of control $\tilde{u}(\tau)$, including the case of fixed control time T.

The proof of Proposition 7 follows from the analysis of the higher-order terms in sliding variation along the extremal trajectory. Calculations result in the following expression:

$$\delta\gamma_i = 2\cos\left(\frac{\xi}{2}\right)\delta\tau_i - \left|\frac{\sin^3\left(\frac{\xi}{2}\right)}{u_{\max}}\right| q_i \delta\tau_i^2 + q_i^{(3)} \delta\tau_i^3 + o(\delta\tau_i^3), \tag{F4}$$

where

$$q_i^{(3)} = \frac{1}{3} u_{\max}^2 \cos\left(\frac{\xi}{2}\right) \left[2\sec^2\left(\frac{\eta}{2}\right) - 3q_i^2 \tan^4\left(\frac{\eta}{2}\right) - 6\cot(\gamma_i)\left(\tan\left(\frac{\eta}{2}\right) + (q_i+1)\tan^3\left(\frac{\eta}{2}\right)\right)\right]. \tag{F5}$$

The necessary condition of the local optimality is thus the inequality $\sum_{i=1}^n q_i \delta\tau_i^2 \geq 0$ in which the variations $\delta\tau_i$ are subject to constraint $\sum_{i=1}^n \delta\tau_i = 0$. The power of sliding variation is in the fact that the quadratic form in the left-hand side of this inequality is diagonal (i.e. the contributions of the sliding variations $\delta\gamma_i$ are independent up to the second order in $\delta\tau_i$). Thus, optimality implies non-negativity of the following simple quadratic form:

$$Q_{kj} = \delta_{kj} q_k + q_n \quad (k, j = 1, ..., n-1), \tag{F6}$$

which can be easily rewritten in the form of statement of Proposition 7.

Appendix G: Proof of Proposition 9

Let $q' = q_{i'} < 0$ be the smallest term in the set $\{q_i\}$. By applying Proposition 7 to the corner points adjacent to i'-th we have: $q_{i'\pm 1} + q_{i'} < 0$. These inequalities can be rewritten after some algebra as

$$\delta\gamma_{i'} > -\frac{\eta}{2} - \arccos\left(\sqrt{\sin^2\left(\frac{\eta}{2}\right)(\cos(\eta)+2)}\right);$$
$$\delta\gamma_{i'} < \frac{\eta}{2} + \cos^{-1}\left(\sqrt{\sin^2\left(\frac{\eta}{2}\right), (\cos(\eta)+2)}\right), \tag{G1}$$

where $\delta\gamma_{i'} = (\gamma_{i'} \mod \pi) - \frac{\pi}{2}$ $(|\delta\gamma_{i'}| < \frac{\pi+\eta}{2})$. One can show that at least one of the inequalities (G1) holds if $|\eta| < \arccos(\sqrt{2}-1)$. From the definition of η it follows that the latter inequality holds for any $u_{\max} > \sqrt{1+\sqrt{2}}$. This means that for this range of controls the i'-th corner point can be only either the left-most or the right-most corner point of time-optimal extremal. Using Fig. 5 one can accordingly improve the estimate for $n_{\max}$: $n_{\max} \leq \left[\frac{|\eta|}{\pi - |\eta|} + 2\right] \leq 2$ for $u_{\max} > \sqrt{1+\sqrt{2}}$ Q.E.D.

Appendix H: Proof of Proposition 10

Suppose that $\tilde{r}_{i'}$ is interior corner point of the globally time-optimal solution. From (23) it follows that $\tilde{r}_{i,x} = \frac{|\tilde{u}_1^+|}{\tilde{u}_1^+} \sin(\zeta_i) \sin(\frac{\xi}{2}) \propto c \sin(\zeta_i)$. where c is some real constant. Since $|\sin(\zeta_{i'})| < \sin(\frac{\pi+\eta}{2})$ and $|\zeta_{i'} - \zeta_{i'\pm 1}| = \frac{\pi+\eta}{2}$ the following inequality holds:

$$\frac{\tilde{r}_{i',x} - \tilde{r}_{i'\pm 1,x}}{\tilde{r}_{i',x}} > 0. \tag{H1}$$

Proposition 3 states that the trajectory curve in vicinity of $\tilde{r}_{i',x}$ should be Λ-shaped (V-shaped) in the case of $\tilde{r}_{i',x} < 0$ ($\tilde{r}_{i',x} > 0$), as shown in Fig. 11. Together with (H1) this means that both left and right adjacent arcs intersect the plane $x = \tilde{r}_{i',x}$ twice and have the second common point $\{\tilde{r}_{i',x}, -\tilde{r}_{i',y}, \tilde{r}_{i',z}\}$. However, the globally time optimal trajectories can not have intersections with themselves. This contradiction proves the statement of Proposition. The associated maximal number of switchings can be directly counted using Fig. 5.

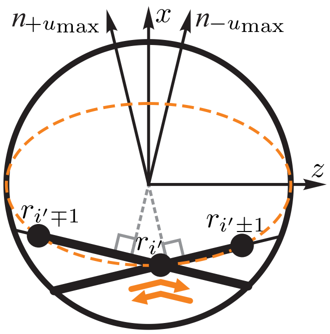

FIG. 11. Projection of the extremal on xz-plane in vicinity of the corner point $\tilde{r}_{i'}$ in the case $\tilde{r}_{i',x}<0$. Orange dashed ellipse is the projection of intersection of the Bloch sphere with the planes $\lambda_{\pm 1}$. Arrows indicates the admissible routes of passing the point $\tilde{r}_{i'}$ according to Proposition 3.

Appendix I: Proof of Proposition 11

The statement of Proposition will be proven by contradiction. Suppose that the first of inequalities (24) is violated (the case of violation of the second inequality can be treated similarly), i.e. $\exists i : (\forall j : \tilde{r}_{i,x}\le\tilde{r}_{j,x}\wedge\tilde{r}_{i,x}<0)$. Using Proposition 3 we conclude that $\tilde{r}_{i,x}\le\tilde{r}_{i-1,x},\tilde{r}_{i+1,x}$ and that the trajectory around $\tilde{r}_i$ is Λ-shaped: $\exists\epsilon,\forall\delta\tau\in(-\epsilon,\epsilon) : \tilde{r}_x(\tilde{\tau}_i{+}\delta\tau){<}\tilde{r}_x(\tau_i)$. Similarly to the proof of Proposition 10, these observations mean that the both arcs $\tau\in(\tilde{\tau}_{i-1},\tilde{\tau}_i)$ and $\tau\in(\tilde{\tau}_i,\tilde{\tau}_{i+1})$ should cross the plane $x{=}\tilde{r}_{i,x}$ twice and thus have the common point $\{\tilde{r}_{i,x},-\tilde{r}_{i,y},\tilde{r}_{i,z}\}$. However, the latter contradicts with the assumed global time optimality of the trajectory $r(\tau)$.

Appendix J: Proof of Proposition 12

Similarly to $\tilde{r}^+$ and $\tilde{r}^-$, let us introduce the new notations $r_\pm{=}\frac{\tilde{r}_1+\tilde{r}_n}{2}\pm\mathrm{sign}(|\tilde{r}_{1,x}|{-}|\tilde{r}_{n,x}|)\frac{\tilde{r}_1-\tilde{r}_n}{2}$ for the first and the last corner points $\tilde{r}_1$ and $\tilde{r}_n$ of trajectory $\tilde{r}(\tau)$, so that $|\tilde{r}_{+,x}|\ge|\tilde{r}_{-,x}|$. Using Fig. 5 we find that

$$n_{\mathrm{I}}{=}\left|\frac{\zeta_+-\zeta_-}{\pi+\eta}\right|+1{=}\left|\frac{\arcsin(\tilde{r}_{+,x}\phi){-}\arcsin(\tilde{r}_{-,x}\phi)}{2\arctan(u_{\max}\phi)}\right|+1, \tag{J1}$$

where $\phi{=}\frac{1}{\sin(\frac{\xi}{2})}$. Eq. (J1) can be rewritten as

$$n_{\mathrm{I}}{=}\frac{\int_0^\phi\left|\frac{\tilde{r}_{+,x}}{\sqrt{1-\phi^2\tilde{r}_{+,x}^2}}-\frac{\tilde{r}_{-,x}}{\sqrt{1-\phi^2\tilde{r}_{-,x}^2}}\right|d\phi}{\int_0^\phi(\frac{u_{\max}}{1+u_{\max}^2\phi^2})d\phi}+1. \tag{J2}$$

The integrands in the numerator and denominator of (J2) are monotonically increasing and decreasing functions of ϕ in the range of interest. Since $\sin(\frac{\xi}{2}){\ge}|\tilde{r}_{+,x}|$ one obtains the upper estimate $n_{\mathrm{I}}{\le}n_{\mathrm{I,max}}$, where

$$n_{\mathrm{I,max}}{=}n|_{\phi=\frac{1}{|\tilde{r}_{+,x}|}}{=}\frac{\arccos(\frac{\tilde{r}_{-,x}}{\tilde{r}_{+,x}})}{2\arctan(\frac{u_{\max}}{|\tilde{r}_{+,x}|})}{+}1. \tag{J3}$$

In order to make this result constructive, we will find the upper estimate for $n_{\mathrm{I,max}}$ by replacing $\tilde{r}_{+,x}$ and $\tilde{r}_{-,x}$ in (J3) with their upper and lower estimates given in Proposition 11: $|\tilde{r}_{-,x}|{<}|\tilde{r}_{+,x}|{<}|\tilde{r}_x^+|$, and $0{<}|\tilde{r}_{-,x}|{<}|\tilde{r}_x^-|$. Elementary analysis shows that $n_{\mathrm{I,max}}(\tilde{r}_{+,x},\tilde{r}_{-,x})$ is a monotonic function of $\tilde{r}_{-,x}$ and reaches a maximum when $\mathrm{sign}(\tilde{r}_{+,x})\tilde{r}_{-,x}$ is minimal. At the same time, $n_{\mathrm{I,max}}(\tilde{r}_{+,x},\tilde{r}_{-,x})$ is a concave function of $\tilde{r}_{+,x}$ when $\tilde{r}_{+,x}\tilde{r}_{-,x}{<}0$ and monotonically increasing function of $|\tilde{r}_{+,x}|$ in the range $\tilde{r}_{+,x}\tilde{r}_{-,x}{>}0$. Using these properties, we obtain inequality (25a) for the case $\tilde{r}_x^+\tilde{r}_x^-{<}0$ and the second of the estimates (25b) for the case $\tilde{r}_x^+\tilde{r}_x^-{>}0$.

Note that the latter estimate directly accounts for the location of only one trajectory endpoint and can be further refined. Namely, due to (24) the corner points in the case $\tilde{r}_{+,x}\tilde{r}_{-,x}{>}0$ are located in the range $\tilde{r}_{i,x}{\in}[0,\tilde{r}_x^+]$. Since the x-coordinates of the corner points are monotonic functions of the index i (see Proposition 10 and Fig. 5), the trajectory can be split into two continuous parts R_1 and R_2 such that all $n_{R_1}(n_{R_2})$ corner points in the segment $R_1(R_2)$ belong to the range $\tilde{r}_{i,x}{\in}(\tilde{r}_x^-,\tilde{r}_x^+]$ ($\tilde{r}_{i,x}{=}[0,\tilde{r}_x^-]$), and their junction point $\tilde{r}_c$ is chosen such that $\tilde{r}_{c,x}{=}\tilde{r}_x^-$. Using these range estimates and the extremal properties of function (J3) we obtain that $n_{R_1}{\le}\frac{\arccos(\frac{\tilde{r}_x^-}{\tilde{r}_x^+})}{|2\arctan(\frac{u_{\max}}{\tilde{r}_x^+})|}{+}1$. Let us show that $n_{R_2}{\le}3$ (which will prove the first estimate in (25b)). Indeed, the duration $\tilde{\Delta\tau}_{R_2}$ of this segment can not exceed π (the maximal duration of the trajectory with $\tilde{u}(\tau){=}0$ connecting $\tilde{r}^-$ and $\tilde{r}_c$). At the same time, according to eq. (19) the minimal duration of each arc of the bang-bang trajectory is $\frac{\pi}{2}\cos\alpha$. Thus, the number of the interior bang segments of duration $\tilde{\Delta\tau}$ in the case $u_{\max}{\le}1$ can not exceed $[2\sqrt{2}]{=}2$, i.e. $n_{R_2}{\le}3$ (the same restriction for the case $u_{\max}{>}1$ trivially follows from Proposition (8)). Hence, Proposition is completely proven.

[1] P. von den Hoff, S. Thallmair, M. Kowalewski, R. Siemering, and R. de Vivie-Riedle, "Optimal Control Theory – Closing the Gap between Theory and Experiment," Phys. Chem. Chem. Phys. **14**, 14460 (2012).

[2] P. De Fouquieres and S. G. Schirmer, "A Closer Look at Quantum Control Landscapes and Their Implication for Control Optimization," Infin. Dimens. Anal. Qu. **16**, 1350021 (2013).

[3] A. N. Pechen and D. J. Tannor, "Are There Traps in Quantum Control Landscapes?," Phys. Rev. Lett. **106**, 120402 (2011).

[4] H. A. Rabitz, M. M. Hsieh, and C. M. Rosenthal, "Quantum Optimally Controlled Transition Landscapes," Science **303**, 1998 (2004).

[5] R. Wu, A. Pechen, H. Rabitz, M. Hsieh, and B. Tsou, "Control Landscapes for Observable Preparation with Open Quantum Systems," J. Math. Phys. **49**, 022108 (2008).

[6] A. Pechen, D. Prokhorenko, R. Wu, and H. Rabitz, "Control Landscapes for Two-Level Open Quantum Systems," J. Phys. A: Math. Gen. **41**, 045205 (2008).

[7] K. W. Moore, A. Pechen, X.-J. Feng, J. Dominy, V. J. Beltrani, and H. Rabitz, "Why Is Chemical Synthesis and Property Optimization Easier than Expected?" Phys. Chem. Chem. Phys. **13**, 10048 (2011),.

[8] C. Brif, R. Chakrabarti, and H. Rabitz, "Control of Quantum Phenomena: Past, Present, and Future," New J. Phys. **12**, 075008 (2009).

[9] T.-S. Ho and H. Rabitz, "Why Do Effective Quantum Controls Appear Easy to Find?," J. Photochemistry Photobiology **180**, 226 (2006).

[10] L. S. Pontryagin, V. G. Boltyanskii, R. V. Gamkrelidze, and E. F. Mishchenko, *The mathematical theory of optimal processes* (John Wiley and Sons, New York, 1962).

[11] A. A. Agrachev, and Y. Sachkov *Control theory from the geometric viewpoint* (Springer Berlin Heidelberg, 2004), Encyclopaedia of Mathematical Sciences, Vol. 87.

[12] M. Lapert, Y. Zhang, M. Braun, S. J. Glaser, and D. Sugny, "Singular Extremals for the Time-Optimal Control of Dissipative Spin 1/2 Particles," Phys. Rev. Lett. **104**, 083001 (2010).

[13] K. D. Greve, D. Press, P. L. McMahon, and Y. Yamamoto, "Ultrafast Optical Control of Individual Quantum Dot Spin Qubits," Rep. Prog. Phys. **76**, 092501 (2013).

[14] Y. Kodriano, I. Schwartz, E. Poem, Y. Benny, R. Presman, T. A. Truong, P. M. Petroff, and D. Gershoni, "Complete Control of a Matter Qubit Using a Single Picosecond Laser Pulse," Phys. Rev. B **85**, 241304 (2012).

[15] F. Schäfer, I. Herrera, S. Cherukattil, C. Lovecchio, F. S. Cataliotti, F. Caruso, and A. Smerzi, "Experimental Realization of Quantum Zeno Dynamics," Nature Communications **5**, 3194 (2014).

[16] N. Malossi, M. G. Bason, M. Viteau, E. Arimondo, D. Ciampini, R. Mannella, and O. Morsch, "Quantum Driving of a Two Level System: Quantum Speed Limit and Superadiabatic Protocols – an Experimental Investigation," J. Phys.: Conf. Ser. **442**, 012062 (2013).

[17] S. N. Shevchenko, S. Ashhab, and F. Nori, "Landau-Zener-Stückelberg Interferometry," Phys. Rep. **492**, 1 (2010).

[18] N. Khaneja, R. Brockett, and S. J. Glaser, "Time Optimal Control in Spin Systems," Phys. Rev. A **63**, 032308 (2001).

[19] A. Pechen and N. Il'in, "Trap-free Manipulation in the Landau-Zener System," Phys. Rev. A **86**, 052117 (2012).

[20] A. N. Pechen and N. B. Ilin, "Existence of Traps in the Problem of Maximizing Quantum Observable Averages for a Qubit at Short Times," Proc. Steklov Inst. Math. **289**, 213 (2015).

[21] V. Jurdjevic and H. J. Sussmann, "Control Systems on Lie Groups" J. Differ. Equ. Appl. **12**, 313 (1972).

[22] D. DAlessandro, "Topological Properties of Reachable Sets and the Control of Quantum Bits," Syst. Control Lett. **41**, 213 (2000).

[23] R. B. Wu, C. W. Li, and Y. Z. Wang, "Explicitly Solvable Extremals of Time Optimal Control for 2-Level Quantum Systems," Phys. Lett. A **295**, 20 (2002).

[24] U. Boscain and Y. Chitour, "Time-Optimal Synthesis for Left-Invariant Control Systems on $SO(3)$," SIAM J. Control **44**, 111 (2005).

[25] G. C. Hegerfeldt, "Driving at the Quantum Speed Limit: Optimal Control of a Two-Level System," Phys. Rev. Lett. **111**, 260501 (2013).

[26] U. Boscain and P. Mason, "Time Minimal Trajectories for a Spin 1/2 Particle in a Magnetic Field," J. Math. Phys. **47**, 062101 (2006).

[27] A. A. Agrachev and R. V. Gamkrelidze, "Symplectic Geometry for Optimal Control," in *Nonlinear Controllability and Optimal Control*, edited by H. J. Sussmann (Taylor & Francis, 1990) Chapman & Hall/CRC Pure and Applied Mathematics, Vol. 133.

[28] A. Agrachev and R. Gamkrelidze, "Symplectic methods for optimization and control," in *Geometry of Feedback and Optimal Control*, edited by B. Jakubczyk and W. Respondek (Marcel Dekker, New York, 1998), Pure And Applied Mathematics, Vol. 207, p. 19.

[29] U. Boscain and B. Piccoli *Optimal Synthesis for Control Systems on 2-D Manifolds*, (Springer, 2004), Mathématiques et Applications, Vol. 43.

[30] B. Goh, "Necessary Conditions for Singular Extremals Involving Multiple Control Variables," SIAM J. Control **4**, 716 (1966).

[31] A. A. Milyutin and N. P. Osmolovskii, *Calculus of Variations and Optimal Control* (American Mathematical Society, Providence, 1998).

[32] A. J. Krener, "The High Order Maximal Principle and Its Application to Singular Extremals," SIAM J. Control **15**, 256 (1977).